

Classification of breast tissue by electrical impedance spectroscopy

J. Estrela da Silva¹

J. P. Marques de Sá¹

J. Jossinet²

¹INEB (Instituto de Engenharia Biomédica), Faculdade de Engenharia da Universidade do Porto, Porto, Portugal

²INSERM (Institut National de la Santé et de la Recherche Médicale), Lyon, France

Abstract—*Electrical impedance spectroscopy is a minimally invasive technique that has clear advantages for living tissue characterisation owing to its low cost and ease of use. The present paper describes how this technique can be applied to breast tissue classification and breast cancer detection. Statistical analysis is used to derive a set of rules based on features extracted from the graphical representation of electrical impedance spectra. These rules are used hierarchically to discriminate several classes of breast tissue. Results of statistical classification obtained from a data set of 106 cases representing six classes of excised breast tissue show an overall classification efficiency of ~92% with carcinoma discrimination >86%.*

Keywords—*Impedance spectroscopy, Tissue characterisation, Data classification, Discriminant analysis, Breast cancer*

Med. Biol. Eng. Comput., 2000, 38, 26–30

1 Introduction

ELECTRICAL IMPEDANCE techniques have long been used for tissue characterisation and in monitoring applications, of which impedocardiography is the best known (KUBICEK *et al.*, 1970). These techniques have also enabled impedance mapping (TACHIBANA *et al.*, 1970; HENDERSON and WEBSTER, 1978) and, more recently, dynamic imaging (BROWN *et al.*, 1994).

Specific impedance (also termed 'impedivity') is the AC equivalent of resistivity for DC current. The specific impedance of a tissue is determined by its electric and dielectric properties, which depend, among other things, on the cell concentration, membrane capacitance, electric conductivity in interstitial space and the intracellular medium (SCHWAN, 1959; FOSTER and SCHWAN, 1989). The easiness, low cost and minimum invasiveness are praised features of the impedance techniques.

In recent decades, electric and dielectric measurements have been carried out in breast tissue under a range of experimental conditions including *in-vivo* or *ex-vivo* measurements and using various measurement techniques (SUROWIEC *et al.*, 1988; MORIMOTO *et al.*, 1990; CAMPBELL and LAND, 1992; HEINITZ and MINET, 1995). In the 488 Hz–1 MHz range, significant differences in the impedivity modulus and phase angle from among six groups of breast tissue were found by one of the authors (JOSSINET, 1998).

These findings suggest that electrical impedance spectroscopy (EIS) is potentially usable for the discrimination of breast tissue and especially for the detection of breast cancer. The present paper describes a method for classifying breast tissues based on EIS. These new results were attained using features derived from the Argand plot of the impedivity data collected in freshly excised tissue. The set of features used comprised those defined in a previous study (JOSSINET and LAVANDIER, 1998)

as well as additional features selected for their discrimination ability. A statistical hierarchical approach was adopted using twelve-point and seven-point spectra.

2 Materials and methods

2.1 Data set

The initial data set consisted of 120 spectra recorded in samples of breast tissue from 64 patients undergoing breast surgery. Each spectrum consisted of twelve impedance measurements taken at different frequencies ranging from 488 Hz to 1 MHz. Details concerning the data collection procedure as well as classification of the cases and frequencies used are given elsewhere (JOSSINET, 1996; JOSSINET, 1998). Prior to any classification attempt, 14 spectra were discarded since they exhibited manifestly abnormal features (erroneous I_0 , low D_A) due to poor tissue collection care and/or data measurement. In the remaining 106 cases, the following six classes of tissue were represented:

Normal tissue classes:	connective tissue (con):	14 cases
	adipose tissue (adi):	22 cases
	glandular tissue (gla):	16 cases
Pathological tissue classes:	carcinoma (car):	21 cases
	fibro-adenoma (fad):	15 cases
	mastopathy (mas):	18 cases

2.2 Bioelectrical features

The classification features were extracted from EIS plots on the Argand plane the co-ordinates of which were the real impedance part (R_s) and the negative of the imaginary impedance part ($-X_s$). Ideally, those plots have the form of circular arcs, as shown in Fig. 1a, due to the underlying physical model (SCHWAN, 1959; FOSTER and SCHWAN, 1989). Such arcs are characterised by three parameters, classically the intercepts with the horizontal axis (low-frequency and high-frequency limit

Correspondence should be addressed to Dr J. P. Marques de Sá; email: jmsa@fe.up.pt

First received 5 July 1999 and in final form 11 October 1999

© IFMBE: 2000

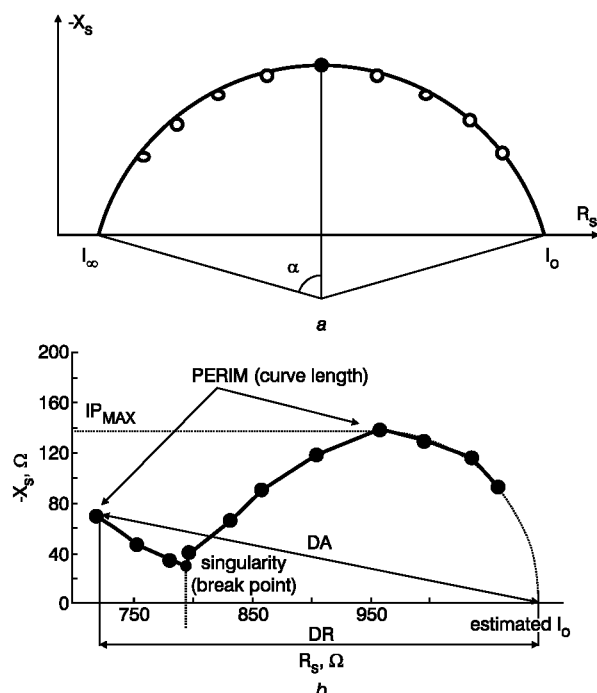


Fig. 1 Impedance locus in Argand plane: a) ideal locus; b) locus example with computed features

resistances, denoted I_0 and I_∞ , respectively) and the fractional power, α , controlling the shift of the centre from the axis. The frequency at which the imaginary part passes by a maximum (IP_{MAX}) characterises the distribution of the frequency points on the arc.

However, due to the various time constants present in the tissues and the limited frequency range, superimposed circular arcs and, generally, incomplete arcs such as the ones shown in Fig. 2 are in practice obtained. In the present study this made it impossible to calculate some of the features derived from the circular arcs (mainly I_∞ and α). Non-conventional features were therefore used.

2.3 Data pre-processing

The objective of the data pre-processing stage was to obtain a group of features capable of characterising of the impedivity loci in the Argand plane. Initially the plots of the various cases in the Argand plane were visually compared. It was expected that obvious distinctions would be found. For instance, the plots of the carcinoma tissues (Fig. 2a) are visually distinct from the plots of the connective tissues (Fig. 2b). Previous reports on excised tissue discrimination (JOSSINET and LAVANDIER, 1998) used the following impedance features, which are shown in Fig. 1b:

I_0	impedivity at zero frequency (low frequency limit resistance)
PA_{500}	phase angle at 500 kHz
S_{HF}	high-frequency slope of phase angle (at 250, 500 and 1000 kHz points)
D_A	impedance distance between spectral ends
BREAK	spectral break point
NOTCH	spectral notch point

In the present study, we also used the following new non-conventional features with a view to achieving a better classification performance than reported previously:

AREA	Area under spectrum
AREA_ D_A	Area normalised by D_A

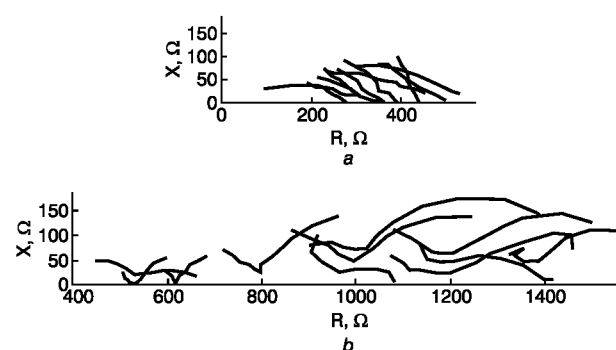


Fig. 2 Argand plots: a) carcinoma tissue samples; b) connective tissue samples

IP_{MAX}	Maximum of the spectrum
D_R	Distance between I_0 and real part of the maximum frequency point
PERIM	Length of spectral curve
SLOPE	Slope of spectral curve obtained by linear regression

All the above features were calculated in Excel 7.0 using programs in Excel's Visual Basic For Applications (VBA) programming language for each of the 106 impedance spectra. PA_{500} , S_{HF} and D_A were directly calculated. The calculation of the remaining features was aided graphically.

2.4 Classification

Given the reduced number of cases representing each class in the available data set, we used a linear discriminant analysis approach to classify the spectra. This seemed to be a sensible choice since the design of linear classifiers is much less demanding in the number of parameters needed to estimate compared to other approaches such as neural nets or K-nearest neighbour classifiers, which are quite demanding in terms of the number of parameters needed to estimate and therefore on the size of the training sets.

Statistical characterisation of the aforementioned set of features was performed in order to assess the features' distribution and discrimination ability. The tool used was STATISTICA 4.5 for Windows (StatSoft®). This characterisation involved normality tests (Kolmogorov-Smirnov, Shapiro-Wilk), discrimination tests (Kruskal-Wallis), inspection of box-and-whisker plots and correlation computations. The Shapiro-Wilk test was used because of its high performance, compared to alternative tests, in the detection of small deviations from normal distribution (SHAPIRO *et al.*, 1968).

The inspection of the box-and-whisker plots and the Kruskal-Wallis test results suggested that a sensible approach to this difficult six-class classification problem was to perform it in two hierarchical stages. The straightforward one-step six-class discrimination (based on the design of six linear discriminant functions) performed quite poorly, as reported in Section 3.2. Hierarchical approaches may be helpful in difficult multiple class separation problems (SWAIN, 1977), which commonly characterise biomedical data.

Based on the discriminative power of the features and the inspection of other statistical results (e.g. scatter diagrams and box-and-whisker plots), a two-stage hierarchical approach was devised as follows.

In the first stage, two groups of class were considered: fatty tissues (adipose and connective tissues) and the other four classes taken together. The second stage involved classifying this four-class group by attempting to split it into the following

categories: carcinoma, fibro-adenoma/mastopathy and glandular tissue. The classification features used were selected by applying the well-known forward stepwise analysis method. A possible third stage could have been the discrimination between mastopathy and fibro-adenoma. However, it was difficult, if not impossible, to reasonably discriminate between these two classes by using the current set of features.

To guarantee acceptable classifier reproducibility, we had to select a low number of discriminating features, assuring a reasonably high dimensionality ratio expressed by the number of cases of the smallest populated class divided by the number of features (FOLEY, 1972; RAUDYS and PIKELIS, 1980). The asymptotic behaviour of the training set and test set error estimates for a linear discriminant classifier suggests that this dimensionality ratio should be three or more in order to obtain reproducible results. For a smaller ratio, there is the risk of over-fitting: the classifier will perform very well in the training set but will behave badly in new cases.

Linear discriminant analysis returns the linear classification functions, which are used to classify new cases. For classifier validation, besides the error estimate obtained for the whole data set, we also performed ten runs designing the classifier with only half of the cases (training set), randomly selected and equally distributed between each group, and testing it using the other half (test set). In this way, we were able to compute average estimates of the training set and test set errors. Splitting the data set in halves enabled a reasonably high dimensionality ratio to be maintained and the variance of the error estimates to be kept at a low level.

3 Results

It was found that normal distribution could not be assumed for all features and all classes. Linear discriminant analysis presupposes that features are normally distributed with equal covariance matrices for all classes. Seldom in nature are these conditions strictly met and it is usually understood that mild deviations are allowable with the penalty that the obtained results are then sub-optimal (FUKUNAGA, 1972). In the present study, the most important features for classification purposes were found to be I_0 , $AREA_{D_A}$ and IP_{MAX} , as reported in Section 3.2. The Shapiro-Wilk test revealed that normality could be assumed for I_0 in adipose and connective tissues ($p < 0.3475$), for $AREA_{D_A}$ in carcinoma ($p < 0.1444$) and for IP_{MAX} in all classes ($p < 0.11$). For other situations, although the Shapiro-Wilk test ruled out normality, the Kolmogorov-Smirnov test accepted it ($p > 0.89$ for all situations), suggesting a mild departure from the normality hypothesis. STATISTICA and other data analysis packages use a pooled covariance matrix, compensating for the fact that covariance matrices may be different for different classes.

Classification experiments were carried out using the full twelve-frequency spectra and truncated spectra consisting of the upper seven points (15.625, 31.25, 62.5, 125, 250, 500 and 1000 kHz) in order to eliminate low-frequency artifacts and measurement errors (GERSING *et al.*, 1995). Identical pre-processing procedures and statistical analyses were applied to both types of spectra.

3.1 Use of full 12-point spectra

For the first classification stage—discrimination of fatty tissues (adipose and connective tissues), the three most discriminative features were found (all with a low Kruskal-Wallis p-level): I_0 , AREA and NOTCH. The classification

results (training set) were 100% correctly classified adipose and connective cases. The contribution of AREA and NOTCH to this performance was marginal.

The second classification stage consisted in discriminating between the three classes of carcinoma, mastopathy/fibro-adenoma and glandular tissue. The classification results (training set) revealed 83.33% correctly classified cases for carcinoma, 78.57% for glandular tissue and 56.25% for the others. The selected features were NOTCH, IP_{MAX} and D_R . No relevant improvement was achieved by using more features.

After performing the described classification experiments with full spectra we established that a more attractive solution could be designed for reduced spectra, as described in the following section. This solution was studied in more detail, particularly with regard to classifier validation.

3.2 Use of seven-point spectra

Spectral truncation did not significantly change the features' values. Their discrimination capability (Kruskal-Wallis results) remained similar to that computed with full spectra, even for the extrapolated I_0 . Table 1 summarises the features' discriminating capability based on the Kruskal-Wallis values. No feature was found to separate mastopathy from the fibro-adenoma and glandular tissue cases. Four features were selected for straightforward six-class classification. Although these features exhibited a low Kruskal-Wallis p-level and low correlation among themselves, the classification performance was relatively poor (Table 2), justifying the proposed two-stage method.

Feature I_0 was found to be sufficient for the discrimination of fatty tissues, achieved for the whole data set with 100% correct classification, with a threshold of $I_0 = 600$. The 95% confidence interval of this 0% error estimate is [0%, 4%] (DUDA and HART, 1973). For normal distributions, the standard deviation of this error estimate is below 0.8% (FOLEY, 1972). Using the evaluation method described in Section 2.4, we obtained an average training set error estimate of $P_{e1} = 3.3\%$ and an average test set error estimate of $P_{e2} = 3.8\%$. The standard deviations of these estimates were respectively 1.1% and 1.2%. The percentage of false negatives was always 0% for both the training and test sets.

If desired, the separation of connective from adipose tissue can also be achieved with similar performance using a threshold of $I_0 = 1600$ (Fig. 3a).

For classification of the non-fatty tissues (carcinoma, fibro-adenoma/mastopathy, glandular tissue), the most discriminating features were: $AREA_{D_A}$ and IP_{MAX} . The classification results were 81.82% for carcinoma, 63.64% for glandular and 75.76% for the others. As can be seen in Fig. 3b, many glandular cases were classified as fibro-adenoma or mastopathy cases. Further experiments have shown that the benefit of adding more features at this second stage was marginal and raised validation issues since the number of cases per class is

Table 1 Spectral features and classes they can help to separate

Feature	Classes it could help to separate
I_0	adi, con, gla + car + fad + mas
PA_{500}	car, adi + con + gla + fad + mas
D_A	car, fad + mas + gla, con + adi
SINGULAR	adi + con, gla + car + fad + mas
$AREA_{D_A}$	car, gla + fad + mas
IP_{MAX}	car, gla + fad + mas
D_R	car, gla + fad + mas
PERIM	adi, con, car, gla + fad + mas

Table 2 Six-class, four-variable classification matrix. Rows: observed classifications; columns: predicted classifications

	Percent correct	Carcinoma	Fibro-adenoma	Mastopathy	Glandular	Connective	Adipose
Carcinoma	81.82	18	0	4	0	0	0
Fibro-adenoma	66.67	1	10	3	1	0	0
Mastopathy	16.67	3	8	3	4	0	0
Glandular	54.54	0	3	7	12	0	0
Connective	85.71	0	0	1	0	12	1
Adipose	90.91	0	0	0	0	2	20
Total	66.37	22	21	18	17	14	21

low. The best that could be assured was the good separation of carcinoma cases from all other cases. This two-class discrimination was achieved using two features: $AREA_{D_A}$ and IP_{MAX} . Table 3 shows that in this way the classification at the second stage was achieved with an overall efficiency of $\sim 92\%$ and carcinoma discrimination of $> 86\%$. The 95% confidence interval of the 8% overall error estimate is [4%, 15%] (DUDA and HART, 1973). For normal distributions, the standard deviation of this error estimate is approximately 2.6% (FOLEY, 1972). Using the evaluation method described in Section 2.4, we obtained an average training set error of $P_{e1} = 8.8\%$ and an average test set error of $P_{e2} = 9.8\%$. The standard deviations of these estimates were, respectively, 4.8% and 6.4%. The average percentage of false negatives was 17.1% for both the training sets and the test sets.

We have also observed that it is possible to adjust the linear boundary by simple translation, as shown in Fig. 3b, improving the false-negative rate to almost 0% with only a minor increase in the false-positive rate (up to a 10% final value).

Table 3 Classification matrix for carcinoma against others (fibro-adenoma + mastopathy + glandular) Rows: observed classifications; columns: predicted classifications

	Percent correct	carcinoma	others
car	86.36	19	3
fad + mas + gla	94.54	3	52
Total	92.21	22	55

4 Discussion and conclusions

Calculating the features used for tissue classification did not require any particular model for the tissue. Using the seven-point spectra (frequency between 15 kHz and 1 MHz), the features that proved to be the most discriminative for the classification of freshly excised breast tissue were I_0 , $AREA_{D_A}$ and IP_{MAX} . The estimated error of the first stage of the proposed two-stage procedure was $\sim 0-3\%$. The estimated error for the second stage was $\sim 8-9\%$ with the possibility of lowering the false-negative rate towards 0% by adjusting the linear boundary. Given the very low number of features used (only one for the first stage and two for the second stage) compared with the lowest number of available cases per class used in the analysis (21 for the carcinoma class), the error estimates obtained are quite accurate, as shown by the confidence intervals, the theoretical bounds for normal distributions and the differences in the average training set and test set error figures as well as their variances.

The discrimination of breast tissue was achieved with an overall classification efficiency of $\sim 92\%$ with carcinoma discrimination of $> 86\%$. All the analyses performed with the present data set led to the conclusion that it is virtually impossible to discriminate with reasonable accuracy between mastopathy, fibro-adenoma and glandular tissues. However, the good results concerning carcinoma discrimination as well as the low cost, ease of use and non-invasiveness of the EIS method suggest that it may be a potential candidate for screening applications in breast cancer detection, the present study yielding a classification method that could be clinically applied.

The results of the present study constitute a major improvement over those obtained in an attempt at carcinoma discrimination reported in a previous work (JOSSINET and LAVANDIER, 1998), respectively 82% overall classification efficiency and 78% for carcinoma discrimination. In this previous work, an empirical scoring equation was employed, using six features ($G_0 = 1/I_0$, PA_{500} , D_A , S_{HF} , presence of a characteristic frequency and presence of a notch point) as inputs, all derived from the entire twelve-frequency spectra. Our method uses a smaller number of measurements (seven-frequency spectra) and a much-reduced number of features (one for the first stage and two for the second stage instead of six), resulting in more reliable and more reproducible results. The use in our study of the impedivity I_0 (instead of the admittivity G_0) together with the

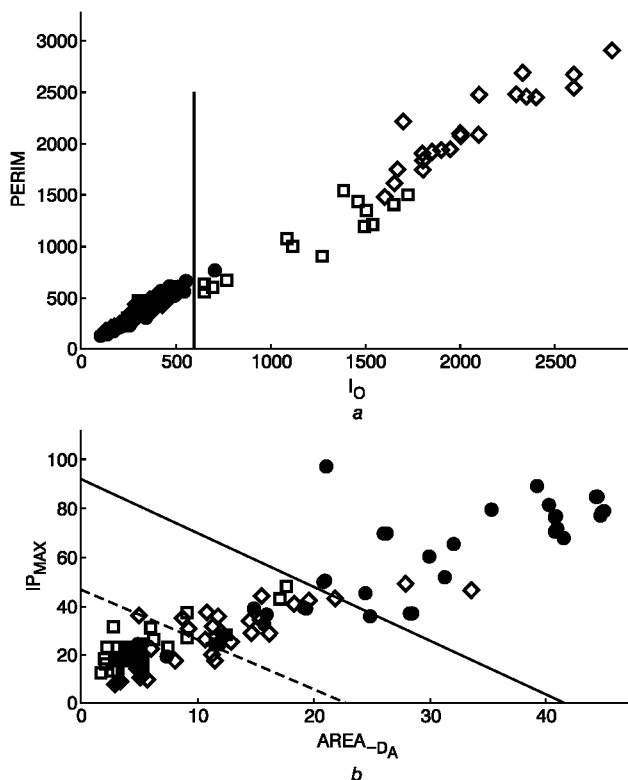


Fig. 3 Scatter plots with classes discriminations (—): a) connective (\square) + adipose (\diamond) against others (\bullet); b) carcinoma (\bullet) against fibro-adenoma + mastopathy (\diamond) + glandular cases (\square). (----) adjusted boundary improving carcinoma discrimination

new features $AREA_{D_1}$ and IP_{MAX} revealed itself to be very important, achieving better results. It is also important to notice that the previous study did not consider the discrimination of groups other than carcinoma, as was done in the present study.

Finally, we wish to stress that our results are only sub-optimal, given that the assumptions for optimal use of a linear discriminant classifier are not entirely verified (as mentioned in the beginning of Section 3). Future collection of more impedance spectroscopic data, a very time-consuming process given the logistic difficulties and clinical protocols needed for completing such a task, may lead in the future to improved tissue class discrimination via the application of more complex classification methods.

References

- BROWN, B. H., BARBER, D. C., MORICE, A.H., and LEATHARD, A. D. (1994): 'Cardiac and respiratory related electrical impedance changes in the human thorax', *IEEE Trans. Biomed. Eng.*, **BME-41**, pp. 729–734
- CAMPBELL, A. M., and LAND, D. V. (1992): 'Dielectric properties of female breast tissue measured *in vitro* at 3.2 GHz', *Phys. Med. Biol.*, **37**, pp. 193–210
- DUDA, R., and HART, P. (1973): 'Pattern classification and scene analysis' (Wiley, New York)
- FOLEY, D. H. (1972): 'Considerations of sample and feature size', *IEEE Trans. Inform. Theory*, **IT-18**, pp. 618–626
- FOSTER, K. R., and SCHWAN, H. P. (1989): 'Dielectric properties of tissues and biological materials: a critical review', *CRC Crit. Reviews Biomed. Eng.*, **17**, pp. 25–104
- FUKUNAGA, K. (1972): 'Introduction to statistical pattern recognition' (Academic Press, New York and London)
- GERRING, E., SCHÄFER, M., and OSYPKA, M. (1995): 'The appearance of positive phase angles in impedance measurements on extended biological subjects' in Proc. 'CAIT Workshop on Electrode-Skin Interface in EIT', *Innov. Techn. Biol. Med.*, **16**, (Special Issue 2), pp. 72–76
- HEINITZ, J., and MINET, O. (1995): 'Dielectric properties of female breast tumors' in Proc. '9th Int. Conf. Electrical Bioimpedance', (University of Heidelberg Press), pp. 356–359
- HENDERSON, R. P., and WEBSTER, J. G. (1978): 'An impedance camera for spatially specific measurements of the thorax', *IEEE Trans. Biomed. Eng.*, **BME-27**, pp. 250–254
- JOSSINET, J. (1996): 'Variability of impedivity in normal and pathological breast tissue', *Med. Biol. Eng. Comput.*, **34**, pp. 346–350
- JOSSINET, J. (1998): 'The impedivity of freshly excised human breast tissue', *Physiol. Meas.*, **19**, pp. 61–75
- JOSSINET, J., and LAVANDIER, B. (1998): 'The discrimination of excised cancerous breast tissue samples using impedance spectroscopy', *Bioelectrochem. Bioenerg.*, **45**, pp. 161–167
- KUBICEK, W. G., PATTERSON, R. P., and WITSOE, D. A. (1970): 'Impedance cardiography as a noninvasive method of monitoring cardiac function and other parameters of the cardiovascular system', *Ann. N.Y. Acad. Sciences*, **170**, pp. 24–732
- MORIMOTO, T., KINOUCHI, Y., IRITANI, T., KIMURA, S., KONISHI, Y., MITSUYAMA, N., KOMAKI, K., and MONDEN, Y. (1990): 'Measurement of the electrical bio-impedance of breast tumors', *Eur. Surg. Res.*, **22**, pp. 86–92
- RAUDYS, S., and PIKELIS, V. (1980): 'On dimensionality, sample size, classification error and complexity of classification algorithm in pattern recognition', *IEEE Trans. Patt. Anal. Mach. Intel.*, **PAMI-2**, pp. 242–252
- SHAPIRO, S. S., WILK, S. S., and CHEN, S. W. (1968): 'A comparative study of various tests for normality', *J. Am. Stat. Ass.*, **63**, pp. 1343–1372
- SWAIN, P. H. (1977): 'The decision tree classifier: design and potential', *IEEE Trans. Geosci. Electronics*, **GE-15**, pp. 142–147
- SCHWAN, H. P. (1959): 'Alternating current spectroscopy of biological substances', *Proc. IRE*, **47**, pp. 1841–1855
- SUROWIEC, A. J., STUCHLY, S. S., BARR, J. R., and SWARUP, A. (1988): 'Dielectric properties of breast carcinoma and the surrounding tissues', *IEEE Trans. Biomed. Eng.*, **BME-35**, pp. 257–263
- TACHIBANA, S., AGUILAR, J. A., and BIRZIS, L. (1970): 'Scanning the interior of living brain by impedography', *J. of App. Physiol.*, **28**, pp. 534–539.

Authors' biographies

JORGE ESTRELA DA SILVA graduated in Electrotechnical Engineering from the Faculty of Engineering, Oporto University in 1998. After a period as research trainee at the INEB (Instituto de Engenharia Biomédica), he is presently researcher at the Faculty of Engineering, Oporto. His current research interest is in the area of data classification and software engineering.

JOAQUIM P. MARQUES DE SÁ is Professor at the Faculty of Engineering, Oporto University, where he graduated and obtained his PhD in Electrotechnical Engineering (1984). He supervises the Signal Processing Group of the INEB (Instituto de Engenharia Biomédica) and is co-author of several systems for physiological signal analysis and diagnosis.

JACQUES JOSSINET is presently a research scientist at INSERM (National Institute for Health and Medical Research). Working in the research unit U281, Lyon, devoted to the detection and treatment of tissue proliferation using physical agents, his present research areas are tissue characterisation, especially using electrical impedance spectroscopy, and the interaction of physical agents in biological media.